Biotechnology and Bioengineering

WILEY

BIOTECHNOLOGY AND BIOENGINEERING

ARTICLE

Enrichment of Full AAV2 Using Multicolumn Countercurrent Solvent Gradient Purification (MCSGP)

Julia M. Müller[1,2] | Tereza Müllerová[1] | Daniela Tobler[1] | Damian Hauri[1] | Richard Plieninger[1] | Yuki Higuchi[3] | Ryosuke Takahashi[3] | Sebastian Vogg[4] | Thomas Müller-Späth[4] | Thomas K. Villiger[1]

[1]Institute of Pharma Technology and Biotechnology, University of Applied Sciences and Arts Northwestern Switzerland, Muttenz, Switzerland | [2]Department of Pharmaceutical Sciences, University of Basel, Basel, Switzerland | [3]YMC CO., LTD., Kyoto, Japan | [4]ChromaCon AG, Zürich, Switzerland

Correspondence: Thomas K. Villiger (thomas.villiger@fhnw.ch)

Received: 15 February 2025 | **Revised:** 14 May 2025 | **Accepted:** 18 May 2025

Funding: This study was supported by ChromaCon AG and YMC CO., LTD.

Keywords: AAV | adeno-associated virus | anion exchange chromatography | continuous purification | full/empty separation | multicolumn countercurrent solvent gradient purification (MCSGP)

ABSTRACT

Adeno-associated viruses (AAVs) are non-pathogenic viruses that have become promising delivery vehicles in cell and gene therapy, with several AAV-based therapeutics receiving approval in recent years. However, a critical challenge is the separation of full and empty viral capsids, as empty capsids lack therapeutic DNA and may compromise product efficacy and safety. This study describes a proof-of-concept of a twin-column multicolumn countercurrent solvent gradient purification (MCSGP) process to enhance the ratio of full to empty capsids during AAV purification. Starting from a batch method with anion exchange chromatography, the process was adapted to continuous operation. The implementation of MCSGP, with six cycles, increased full capsid content in the final product pool from 30% to 68% (ddPCR) and 27% to 61% (cryo-TEM) respectively. Moreover, MCSGP was capable of overcoming the inherent yield-purity trade-off in the polishing step by enhancing full capsid recovery. Additionally, the MCSGP process improved productivity by up to 23% and reduced buffer consumption up to 27% compared to the batch method (ddPCR). The increased productivity and reduced buffer consumption offer both economic and environmental benefits. This study demonstrates the potential of MCSGP to meet the rising demand for high-quality AAV products in gene therapy.

1 | Introduction

In recent years, an increasing number of recombinant adeno-associated virus (AAV) based therapeutics have advanced to clinical phases, amplifying the demand for intensified and productive production processes (FDA 2010; Issa et al. 2023; Jungbauer 2013; Penaud-Budloo et al. 2018). One promising approach to increase the efficiency of AAV manufacturing is continuous bioprocessing. While continuous processing is already widely used for well-established production platforms such as those for monoclonal antibodies (Coolbaugh et al. 2021; Ramos et al. 2023), AAV production remains challenging due to the structural complexity of the product and a limited technical repertoire (Moleirinho et al. 2020). Despite this complexity, recent studies have proven that the implementation of continuous manufacturing in AAV

Abbreviations: AAV, adeno-associated virus; AEX, anion exchange chromatography; ASSB, assay buffer; BTP, Bis-tris propane; cGMP, current good manufacturing practice; CIP, cleaning-in-place; CMV, cytomegalovirus; cp, capsid particles; Cryo-TEM, cryo-transmission electron microscopy; CsCl, caesium chloride; CV, column volumes; ddPCR, digital droplet polymerase chain reaction; EGFP, enhanced green fluorescent protein; ELISA, enzyme-linked immunosorbent assay; HEK293F, human embryonic kidney 293 cells; MCSGP, multicolumn countercurrent solvent gradient purification; MP, mass photometry; MWCO, molecular weight cut-off; PBS, phosphate buffered saline; PEI Max, polyethylenimine max; pI, isoelectric point; P/S, product – strong impurity; TMAC, tetramethylammonium chloride; UC, ultracentrifugation; UV, ultraviolet; vg, vector genomes; WPRE, woodchuck hepatitis virus posttranscriptional regulatory element.

production is feasible (Henry et al. 2004; Mendes et al. 2022; Mendes et al. 2022; Park et al. 2024).

During the production of AAVs, various nontherapeutic particles can be created in addition to the functional full AAV particles. The particles can encapsulate diverse versions of the truncated transgene, contaminant DNA derived from the production process, carry an excess genetic material or even be devoid of any cargo (Ebberink et al. 2022; Gimpel et al. 2021; O'Connor et al. 2019; Penaud-Budloo et al. 2018). These variants in the final drug decrease therapeutic activity and potency, increase immunogenicity and potentially cause harmful immunotoxic reactions (Arjomandnejad et al. 2023; Gimpel et al. 2021; Jarvi et al. 2024; Wright 2014). Therefore, their presence must be tightly controlled and minimized to ensure patient safety (FDA 2010; Gimpel et al. 2021; Tanaka et al. 2020; Wright 2014).

AAVs have been used and purified on a laboratory scale for decades, with the most common method being density gradient ultracentrifugation (UC) using caesium chloride (CsCl) or iodixanol (Hermens et al. 1999; Zolotukhin et al. 1999). This approach enables the separation of full, empty, and partially filled capsids, regardless of the capsid's composition (Grieger et al. 2006; Lam et al. 2023; Lock et al. 2010; Strobel et al. 2015). Despite achieving a satisfactory full/empty separation with UC, the method has a low scalability, is time-consuming, and equipment dependent and thus the separation of full and empty capsids for commercial production remains challenging. In addition, CsCl raises toxicity concerns, and iodixanol may induce allergic responses in individuals who are allergic to iodine-based compounds (El Andari and Grimm 2021; Wada et al. 2023). Despite some efforts to make the UC more suitable for larger volumes (Chen 2015; Lock et al. 2010; Wada et al. 2023), industry is seeking alternative, more scalable methods to the traditional separation by ultracentrifugation (Jiang and Dalby 2023; Moleirinho et al. 2020).

Chromatographic purification strategies represent alternative approaches for the separation of empty and full AAV particles, with anion exchange chromatography (AEX) being the most widely utilized method. This approach leverages the slight difference in isoelectric points (pI) between full AAV particles (pI ~5.9) and empty capsids (pI ~6.3) to effectively remove undesired species and enrich the population of full recombinant AAV (Qu et al. 2007; Urabe et al. 2006; Venkatakrishnan et al. 2013). AEX offers a scalable and robust alternative suitable for implementation within a current good manufacturing practice (cGMP) environment for biomanufacturing processes. However, due to the minute difference in pI, baseline separation is generally not achieved by conventional gradient elution, leaving the isolation of full AAV particles a major challenge in the AAV production process (Wright 2008). Instead of a linear gradient, a discontinuous gradient or sequential isocratic steps can be employed to improve the separation between empty and full particles (Hejmowski et al. 2022; Lavoie et al. 2023; Qu et al. 2007; Rieser et al. 2021). However, these methods are generally less robust than linear gradient chromatography as they are susceptible to subtle fluctuations in buffer composition resulting from variations in the manufacturing process across different production lots. As a result, the difficulty of effectively separating certain product-related impurities from the target molecule leads to an inherent trade-off between yield and product purity. An alternative approach proposed to address this challenge is multicolumn countercurrent solvent gradient purification (MCSGP) (Fu et al. 2023). MCSGP has demonstrated considerable advantages in the purification of complex mixtures containing diverse therapeutic substances, such as monoclonal antibodies, peptides, and oligonucleotides (Luca et al. 2020; Müller-Späth et al. 2010; Weldon et al. 2022). This method effectively mitigates the trade-off between product yield and purity while enhancing the utilization of both buffers and resins.

Therefore, the aim of this study is to demonstrate a proof-of-concept for the application of the MCSGP technique for the separation of full and empty AAV particles. Batch anion exchange chromatography (AEX) with linear gradient elution was initially employed to achieve partial separation of empty and full AAV2 serotype particles. A detailed analysis of the elution profile for both particle types facilitated the development of a recycling protocol, which was subsequently integrated into a continuous twin-column chromatography protocol to optimize the recycling process and define the product collection window. The application of MCSGP enabled full AAV particles enrichment in the collected pool with high yields, while simultaneously reducing buffer consumption and improving overall productivity through optimized time scheduling. To the best of our knowledge, this represents the first demonstration of preparative AAV purification using MCSGP, illustrating the potential for continuous countercurrent twin-column purification to be effectively applied to viral vectors.

2 | Materials and Methods

2.1 | AAV Production

HEK293F cells (Viral Production cells 2.0, Thermo Fisher) were cultivated in HyClone Peak Expression Medium (Cytiva) and expanded in shake flasks in an incubator (Multitron, Infors HT, Bottmingen, Switzerland). Cells were transferred to bioreactors (Labfors 5, Infors HT, Bottmingen, Switzerland) and inoculated with a seeding density of 1.5×10^6 cells/mL with a total volume of 1.2 L. After reaching a cell density of 3×10^6 cells/mL, the cells were transiently transfected with three plasmids pHelper (pAdDeltaF6), pRepCap (pAAV2/2), and pCMV-EGFP (pAAV. CMV. PI. EGFP. WPRE.b) that were purchased from Addgene and previously amplified in-house. For the transient transfection, 1 μg of total plasmid DNA per million cells was mixed in a molar ratio of 0.5:2:1, and subsequently complexed using polyethylenimine Max (PEI Max, Polysciences) in a 2:1 ratio (total of 10% of the culture volume). Following the transfection, the cells were cultivated for 3 days before harvesting.

2.2 | Harvest and Depth Filtration

The cells were lysed directly in the bioreactor by the addition of Tween-20 (Sigma, P1379) to a final concentration of 0.5% (v/v)

and incubated for 1 h at 37°C and 250 rpm. Subsequently, the pH was adjusted to 7.4 with $NaHCO_3$ (Sigma, 1.06323), followed by the addition of $MgCl_2$ (Sigma, M0250) to a final concentration of 2 mM and benzonase to 50 U/mL (Merck, 1016560001). The nuclease digestion was carried out at 37°C for 2 h at 250 rpm. Afterwards, 400 mM NaCl (Sigma, S9625) were spiked into the harvest to stabilize the AAVs. The viral suspension was then centrifuged at 1000 g and 18°C for 1 h. The harvest was clarified by depth-filtration (SUPRAcap 50, 2–20 μm, SC050PDK11, Cytiva), followed by a bioburden reduction filtration (Mini Kleenpak Capsule, 0.2 μm, KM5EAVP2S, Cytiva).

2.3 | Chromatography Equipment

Preparative chromatography experiments were performed using Contichrom® CUBE 30 equipment (ChromaCon AG, Zurich, Switzerland) in combination with the ChromIQ® operating software. All chromatography experiments were performed at room temperature. Conductivity, pH and UV detection at 260 and 280 nm were monitored online. One UV detector with a pathlength of 0.5 mm was installed at the outlet of each column.

2.4 | Batch Affinity Chromatography Method

For the AAV capture, a POROS CaptureSelect AAVX (5 × 50 mm, Thermo Fisher) column was equilibrated with 15 column volumes (CV) of equilibration buffer (50 mM Tris-HCl (Sigma, 10708976001), 300 mM NaCl, 0.01% (w/v) poloxamer 188 (Thermo Fisher Scientific, J66087.36), pH 8) before loading the clarified AAV2 harvest onto the column. After loading, the column was washed with 15 CV of equilibration buffer. The product was eluted in 10 CVs using a low pH elution buffer (100 mM glycine (Carl Roth, 3187.5), 240 mM arginine (Carl Roth, 3144.2), 200 mM NaCl, 0.01% (w/v) poloxamer 188, pH 2.5) and directly neutralized with 12% v/v neutralization buffer (1 M Tris-HCl, pH 10). The column was regenerated using 7.5 CVs strip buffer (2 M NaCl), followed by 7.5 CV 1 M acetic acid (Carl Roth, 6755.3) and a 7.5 CV 6 M guanidine-HCl (Thermo Fisher Scientific, A13543 .0B) CIP in reverse flow direction. Equilibration, wash, and elution were performed at 300 cm/h, loading at 100 cm/h, and stripping and cleaning at 150 cm/h.

2.5 | Batch Polishing Chromatography

All AAV purification experiments were performed on an AEX column designed with large pores for virus purification: MacroSep IEX Q (100 × 4.6 mm, 900 nm, 30 μm, YMC, Japan). The column was equilibrated with 15 CVs of equilibration buffer (20 mM BTP (Sigma, B6755), 2 mM $MgCl_2$, 1% (w/v) sucrose (Sigma, S9378), 0.1% (w/v) poloxamer 188, pH 9.0) before loading the diluted AAV2 capture eluate onto the column. The AAV2 capture eluate was diluted by continuous addition of equilibration buffer to a final conductivity of 4.8 mS/cm (9.5-fold dilution). A batch chromatography run with a high load density of 1.09×10^{16} cp/L resin was performed to have sufficiently high titers for the subsequent offline mass photometry analysis of the individual fractions. Another design batch run, using the same load material as for the MCSGP run, was performed with a load density of 2.47×10^{15} cp/L resin. Due to material limitations a relatively low loading density was chosen for this proof-of-concept study. After loading, the column was washed with 15 CVs of equilibration buffer. The elution was performed with a linear gradient from 15% to 50% elution buffer (20 mM BTP, 2 mM $MgCl_2$, 500 mM choline chloride (Sigma, C1879), 1% (w/v) sucrose, 0.1% (w/v) poloxamer 188, pH 9.0) over 16.5 CVs. The column was stripped with 100% elution buffer for 10 CVs, followed by a 10 CV CIP with 1 M NaOH and neutralization for 10 CV using 1 M NaCl. A flow rate of 361 cm/h was used for every step.

2.6 | Multicolumn Countercurrent Solvent Gradient Purification (MCSGP)

For the MCSGP run, two columns (MacroSep IEX Q, 100 × 4.6 mm, 900 nm, 30 μm, YMC, Japan) were operated in a cyclic manner switching in between interconnected and batch phases. In the start-up phase, the first column was pre-fed with diluted AAV2 capture eluate (conductivity 4.6 mS/cm) to a load density 1.98×10^{15} cp/L resin before moving into the cyclic phase. This phase started with a linear gradient elution from 15% to 50% elution buffer. The first weakly adsorbing fraction (empty particles) was discarded, and the second fraction containing a mixture of empty and full AAV2 particles was recycled and inline diluted before being loaded onto the second column in an interconnected state. Once the recycling was finished, the valves switched back from the interconnected to the parallel operation, where the next, full AAV2 particle fraction was collected while the second column was continued to be loaded with fresh feed (80% of startup load volume) and was washed accordingly. The linear gradient was operated throughout the phases of discarding of empty particles, internal recycling and product elution. Generally, the design of the MCSGP process followed the approach presented by Steinebach (Steinebach et al. 2017). However, in contrast to the conventional MCSGP scheduling, product collection was continued until the end of the elution phase since no recycling of a strongly adsorbing fraction was applied, followed by the column regeneration and re-equilibration phase (Figure 1) to complete the first switch. This rearrangement allowed to minimize column holds in comparison to the conventional MCSGP setup for this binary AAV2 separation. After the first switch, the columns changed their relative position in the second switch and the sequence of tasks was repeated to complete one cycle. A total of 6 cycles were performed, corresponding to 12 column elutions, followed by a shut-down protocol to elute the last AAVs in a single elution.

2.7 | Capsid Titer Measurement by ELISA

Quantitative AAV capsid detection was performed using the ELISA kit (PROGEN AAV2 Titration ELISA 2.0 R) according to the manufacturer's instructions. Samples were diluted in 1 x assay buffer (ASSB) using empirically determined dilution factors to ensure that the capsid concentration remained within

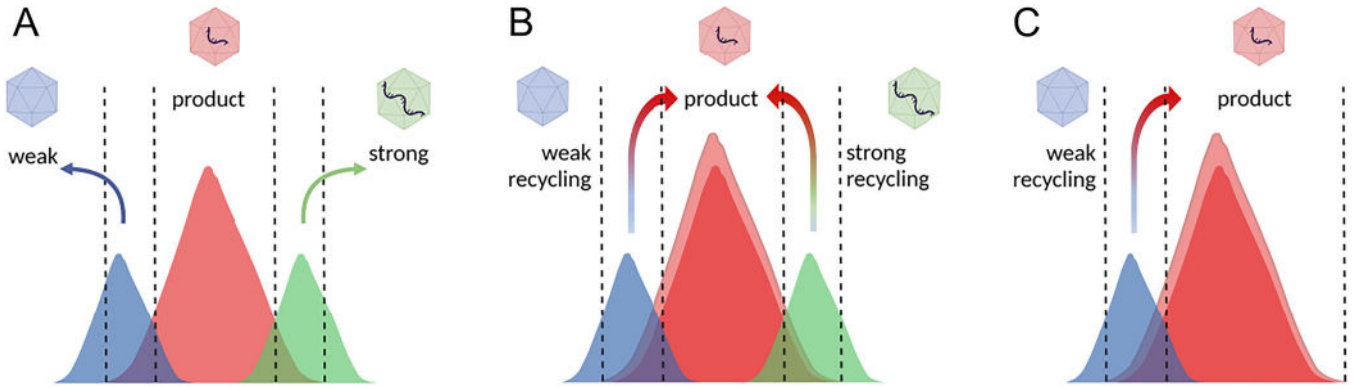

FIGURE 1 | Schematic representation of the impurity separation in the AAV polishing. (A) Batch chromatog-raphy, in which the weakly and strongly adsorbing impurity fractions are discarded. (B) MCSGP with ternary purification. The overlapping regions of the weakly adsorbing impurities (empty AAVs) and strongly ad-sorbing impurities (overfilled AAVs) with the product (full AAVs), respectively, are recycled during the process. (C) In our case of AAV2 with EGFP, we only observed empty and full without any partial nor overfull particles. Therefore, a binary separation of the empty and full particles was performed using the MCSGP technique, only recycling the weakly adsorbing impurity (empty AAVs) and product (full AAVs) overlapping region. Created in BioRender. Müller, J. (2025) https://BioRender.com/d50r418.

the range of the standard curve. Samples with low expected capsid concentration (5.0×10^8 to 5.0×10^{11} cp/mL) were diluted using a dilution factor of 1- and 200-fold, whereas samples with a high expected capsid concentration (1.0×10^{10} to 1.0×10^{13} cp/mL) were diluted using factors between 500- to 2000-fold. The signal was acquired using a microplate reader (BioTek, Epoch 2) at a UV wavelength of 450 nm.

2.8 | Genome Titer Quantification by Droplet Digital Polymerase Chain Reaction (ddPCR)

The genome copy number evaluation by ddPCR was performed according to the supplier's protocol (Bio-Rad Bulletin 7407 Ver A) if not further specified. The unencapsulated DNA was removed by using DNase digest. For that a total of 40 µL reaction was prepared including 4 µL of sample, 24 µL DNase free water, 4 µL 10 x Pluronic F-68 solution, 4 µL DNase I (10 U; M0303S NEB, Ipswich USA) and 4 µL of 10 x DNase I Reaction Buffer. This was followed by incubation at 37°C for 30 min then held at 4°C. The DNase treated samples were then diluted in 10 x series considering the optimal detection range of the used QX600 (Bio-Rad, Hercules, USA). The capsids were then lysed at 95°C for 10 min and placed on hold at 4°C. For the PCR reaction, Supermix for Probes (No dUTP) was used. Following primers were used for the quantification of the GFP gene: 5′ -ACCACTAC CAGCAGAACACC -3′ (forward), 5′- GACTGGGTGCTCAGGT AGTG -3′ (reverse) and the probe sequence 5′- CCGTGCTGCT GCCCGACA -3′ for FAM (fluoresceine).

2.9 | Cryo-Transmission Electron Microscopy (Cryo-TEM)

A 4 µl aliquot of virus sample was adsorbed 10 s onto a glow-discharged (20 mA, 60 s to render the carbon film hydrophilic, Qorum, UK) holey carbon-coated grid (Lacey, Tedpella, USA), blotted 4 s with Whatman grade 1 filter paper and vitrified into liquid ethane at – 180°C using a Leica GP2 plunger (Leica microsystems, Austria). The Leica chamber was set to 10°C and 90% humidity. Frozen grids were transferred onto a Talos 200 C Electron microscope (FEI, USA) operating at 200 KV. Micrographs were collected on CETA CMOS detector from Gatan using low dose system (40 e-/Å2) at a magnification of 92'000 x corresponding to 1.6 Å per pixel on the image. Defocus values were − 2 to − 3 µm.

To determine the quantity of empty and full capsids, a total of 200 particles were counted manually. For the yield calculation based on the cryo-TEM results, the full AAV content/mL was calculated using the ELISA titer and the % full AAV content as determined by cryo-TEM.

2.10 | Mass Photometry

Before the mass photometry (MP) measurements, polished eluate fractions were concentrated using Amicon Ultra 0.5 centrifugal filters (100 kDa MWCO). The samples were measured on a TwoMP mass photometer (Refeyn Ltd.) using the AquireMP software (2.1). To find the focus, 10 µL of 1 x PBS buffer was pipetted on the gasket. Once the focus was set, 10 µL of the pre-diluted (1:10 in 1 x PBS) sample was applied and mixed with the PBS on the gasket (final dilution of 1:20). Finally, the sample was imaged for 180 s and evaluated in the DiscoverMP software (2.1).

3 | Results and Discussion

The titers of AAV2 produced in HEK293F suspension cells by transient triple transfection ranged from 6.0×10^9 – 5.0×10^{11} cp/mL. The viral particles were harvested through cell lysis followed by centrifugation, depth filtration and a 0.22 µm bioburden reduction filtration and finally pooled, resulting in a pool of 17.9 L and 1.0×10^{14} total viral particles. Subsequently, affinity capture chromatography was performed with an immediate neutralization of the eluate, which was then diluted

to a conductivity of 4.6 mS/cm with equilibration buffer before AEX chromatography.

First a batch polishing method needed to be established, that served as a basis for designing the MCSGP method. Similar to other AEX-chromatography processes (Kurth et al. 2024; Lavoie et al. 2023; Nass et al. 2018; Qu et al. 2007; Urabe et al. 2006), the used MacroSep IEX Q resin with a quaternary ammonium structure was used. As for the mobile phases, a bis-tris propane (BTP) buffer in combination with magnesium chloride at pH 9.0 is commonly used for the AAV polishing and demonstrated to positively influence the separation efficiency of empty and full AAV particles (Dickerson et al. 2021; Gagnon et al. 2021; Hejmowski et al. 2022; Wang et al. 2019) and stability (Khanal et al. 2023; Wright et al. 2005). The quaternary ammonium structure containing salt choline chloride was used in the eluent since it is nontoxic as compared to the commonly used tetramethylammonium chloride (TMAC) and was shown to efficiently separate empty and full particles in combination with a AEX Q-type resin (Kurth et al. 2024). After an initial screening for the mobile phases (data not shown), 20 mM BTP, 2 mM $MgCl_2$, 1% (w/v) sucrose, 0.1% (w/v) poloxamer 188, pH 9.0, with 500 mM choline chloride in the eluent, performed best and was therefore chosen for the subsequent experiments. The batch process was optimized until a partial separation of the empty and full AAV2 particles, as indicated by the UV260/280 ratio (Figure 2C), was obtained.

Since the UV absorption signal obtained by the AAV particles is very small, a time-based approach for the product recycling and collection was chosen instead of UV-based dynamic process control using UV-thresholds. To be able to set the correct time windows, the distribution of full and empty particles in the eluted double peak needed to be determined. For this purpose, a batch chromatography run with a 4.4 times higher loading density was performed and individual fractions of the eluted double peak were collected. A higher loading density was targeted to ensure that the capsid particle titer in the individual fractions was high enough for the subsequent analysis by MP (Figure 2B). The samples were analyzed offline by MP to determine their full AAV content. This data was then used to identify the transition zone from a lower to a higher full AAV %, that is, the fraction where the empty and full particle peaks are expected to be overlapping. The MP data was further compared to the observed UV260/280 ratio of the online data (Figure 2A). As for the MP measurements, a sharp transition from a lower to a higher UV260/280 ratio was observed where the overlap of empty and full AAVs is expected. The transition zone observed by both techniques, the offline MP and online UV-ratio measurements, were in good agreement (Figure 2A,B). While the UV ratio provides only a general indication, it is not considered the most accurate method for determining the full/empty particle content, as it is susceptible to absorption bias and prone to slight deviations, particularly when dealing with low absolute UV values. However, it has proven to be reliable in identifying the transition zone, where the empty and full particles co-elute, as indicated by a fast transition from a lower to a higher UV260/280 ratio. Confirming the transition with offline MP analysis (Figure 2B) shows that this quick method is useful for verifying the recycling, even if the exact full/empty values lack precision. This online UV260/280 ratio data and the offline MP data were used to deduce the transition zone, that is, the overlapping full/empty recycling window, the "weak out" elution windows (removal of empty AAV capsids), and the product collect window (Steinebach et al. 2017).

Before moving to the design of the MCSGP, the correct recycling strategy was confirmed in a design batch run using the same load as for the subsequent MCSGP run. The online UV260/280 ratio from the design batch run showed a good correlation to the previously set recycling windows (Figure 2C).

In this study, only a binary separation between the empty (weakly adsorbing impurity) and full (product) AAV2 particles was performed with only one recycling step. This step corresponds to the part of the chromatogram where the empty and full particles overlap (Figure 1). This modification allowed for a rearrangement of the conventional MCSGP sequence, which typically includes a second recycling window at the product-strong impurity side. In the conventional setup, column 1 goes through the elution phase (weak out, weak recycling, product collection, strong recycling, strong out) while column 2 is regenerated, accepts the recycling, and is then continued to be fed and washed (Steinebach et al. 2017). In our case of AAV2 purification, this classical approach leads to a disproportion of the run duration between the two columns for a switch, as the regeneration and feeding lasts much longer in comparison to the gradient elution phase. By omitting the strong recycling, column 1 can directly proceed to the column regeneration protocol after product collection (Figure 3). This allowed us to parallelize more of the steps between the two columns, significantly reducing the switch time. This novel approach for binary MCSGP separation can significantly reduce the overall processing time and is particularly advantageous for pools with low product concentration, which are commonly found in viral vector processing. In our case, the cycle time was reduced from 220 to 158 min, a reduction of process time of almost 30%. Overall, the entire MCSGP run could be reduced from 1615 to 1124 min.

Based on the batch data, the MCSGP run was designed using the MCSGP wizard tool of the ChromIQ software. Since the design significantly differed from the classical design, the tool was mainly used to determine the phase lengths and flow rates (i.e., gradient- and inline-dilution flow rates) but was programmed manually. The detailed settings for both, the batch and the MCSGP run, can be found in Table 1.

The MCSGP was run for a total of six cycles (Figure 4A,B). In the start-up phase, column 1 was pre-fed and in the shut-down phase, a final batch elution was performed to recover the last AAV particles (Figure 4A). Each of the cycles consists of two switches. In the first switch, the product is eluted from column 1, and in the second switch, from column 2. The overlay of the switches (Figure 4C for switch 1; Figure 4D for switch 2) shows that the two columns are very comparable, showing a highly similar elution profile and retention times. This was especially important in the time-based MCSGP setting, since small shifts in the elution pattern can have a significant impact on the performance. For both switches, the height of the peak is slightly increasing over time. This indicates that more material is entering the system by re-feeding and recycling than is leaving the system.

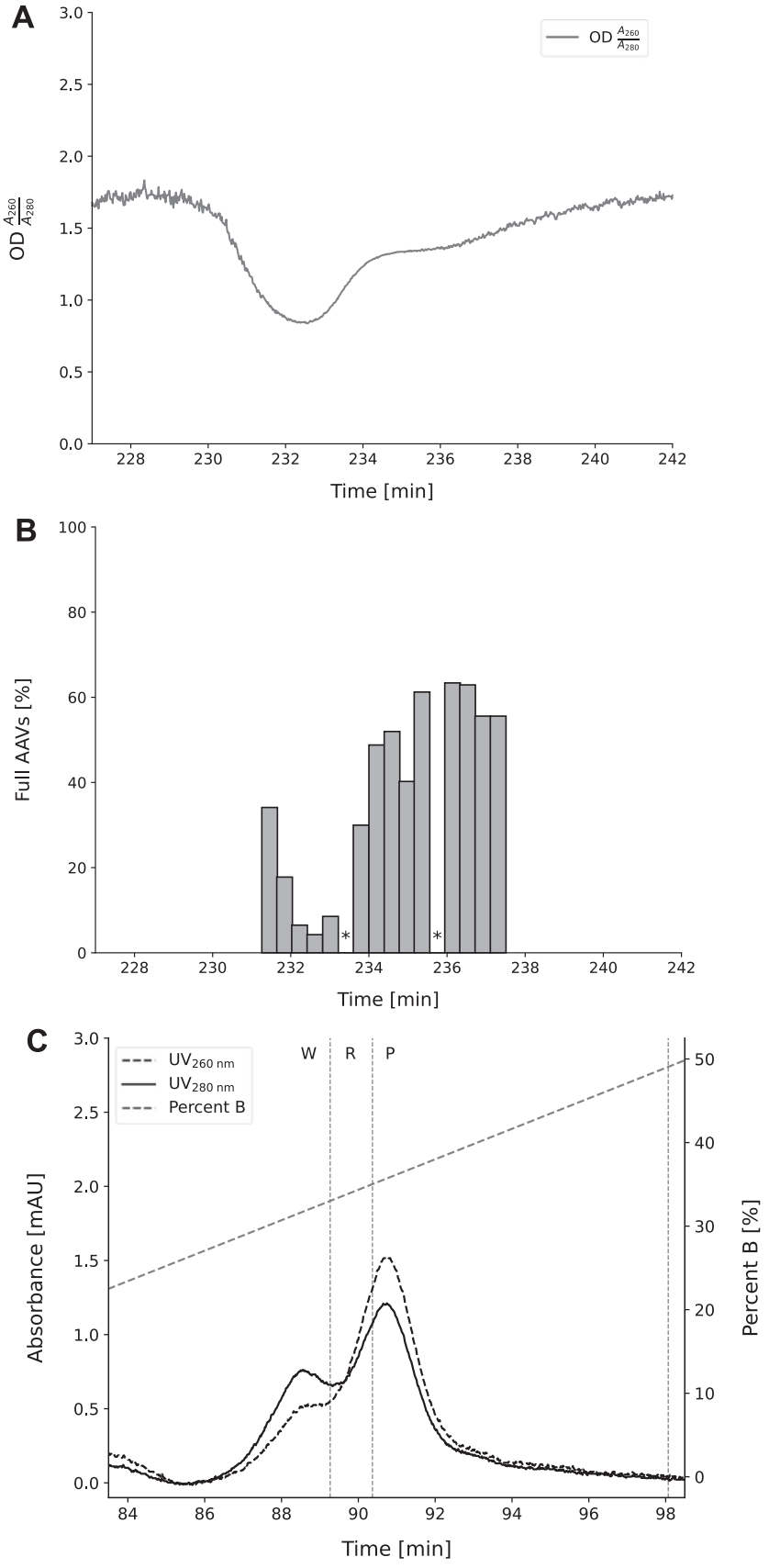

FIGURE 2 | High load density batch run and design batch run for the empty and full AAV2 separation. (A) UV 260/280 ratio of the high load density run. (B) MP data [% full] of the individual fractions collected during the high density load run. * indicate fractions where no valid MP measurement was obtained. (C) UV signals of the design batch run W: weakly adsorbing impurity out; R: recycling; P: product collection.

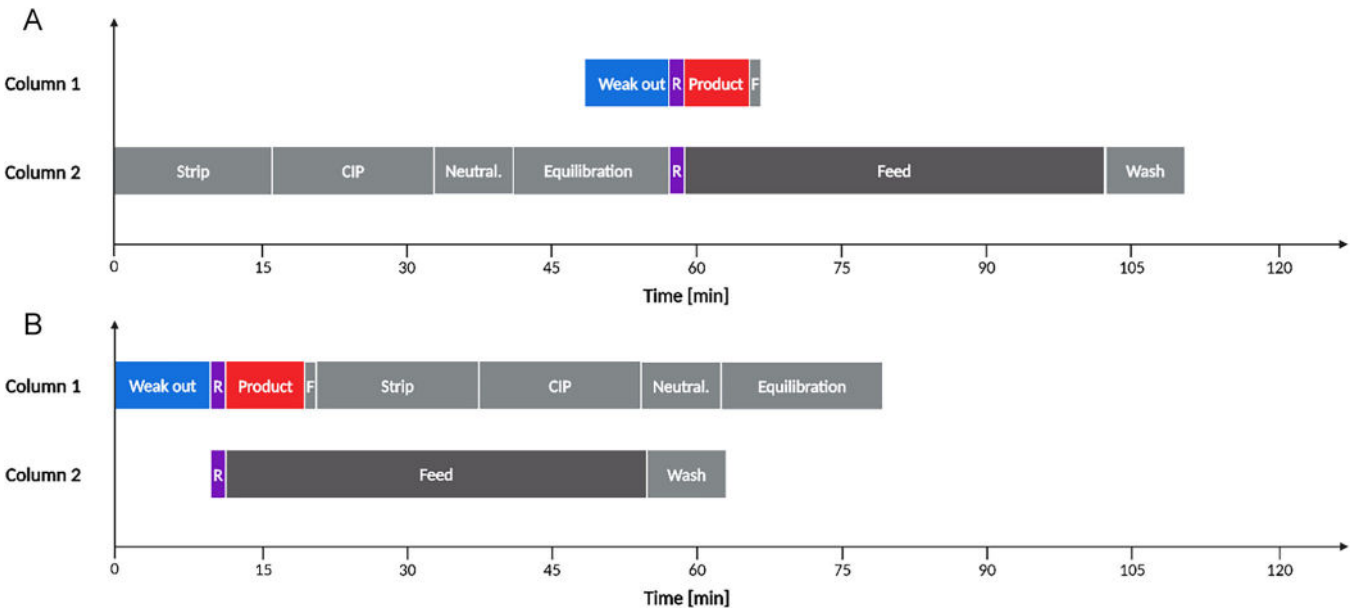

FIGURE 3 | Time schedule of the phase sequence for column 1 and 2 during the MCSGP operation. (A) Con-ventional set-up of phases for a switch used in MCSGP. (B) Adjusted set-up for the phases applied in the MCSGP for the binary separation of empty and full AAVs. R: recycling phase; F: flush mixer. Created in BioRender. Müller, J. (2025) https://BioRender.com/d50c846.

TABLE 1 | Process parameters overview – batch versus MCSGP.

Parameters	Units	High load batch	Design batch	MCSGP
Cycle time	[min]	314	162	158
Total resin volume	[mL]	1.662	1.662	2 ×1.662
Equilibration	[CV]	10	10	10
Equilibration	[cm/h]	361	361	361
Load density (ELISA)	[cp/L resin]	1.09×10^{16}	2.47×10^{15}	1.98×10^{15}
Load density (ddPCR)	[vg/L resin]	—	1.49×10^{15}	5.97×10^{14}
Load density (Cryo-TEM)	[full AAVs/L resin]	—	6.73×10^{14}	5.38×10^{14}
Load flow rate	[cm/h]	361	361	361
Wash length	[CV]	5	5	5
Wash flow rate	[cm/h]	361	361	361
Gradient start - end	[% B]	15 – 50	15 – 50	15 – 50
Gradient length	[CV]	11.55	11.55	11.55
Elution flow rate	[cm/h]	361	361	361
In-line dilution flow rate	[cm/h]	—	—	722
Strip length	[CV]	10	10	10
Strip flow rate	[cm/h]	361	361	361
CIP length	[CV]	10	10	10
CIP flow rate	[cm/h]	361	361	361
Neutralization length	[CV]	5	5	5
Neutralization flow rate	[cm/h]	361	361	361

During process design, the recycling volume was reduced to avoid excessive accumulation. The amount by which the re-loading volume was reduced was estimated based on the total AAVs and the relative peak area of the full AAVs. However, cryo-TEM showed that probably too many full AAVs were re-cycled. It had been estimated that the overlapping region of the chromatogram to be internally recycled would contain 20% of the full particles. Cryo-TEM analysis of the recycled fraction

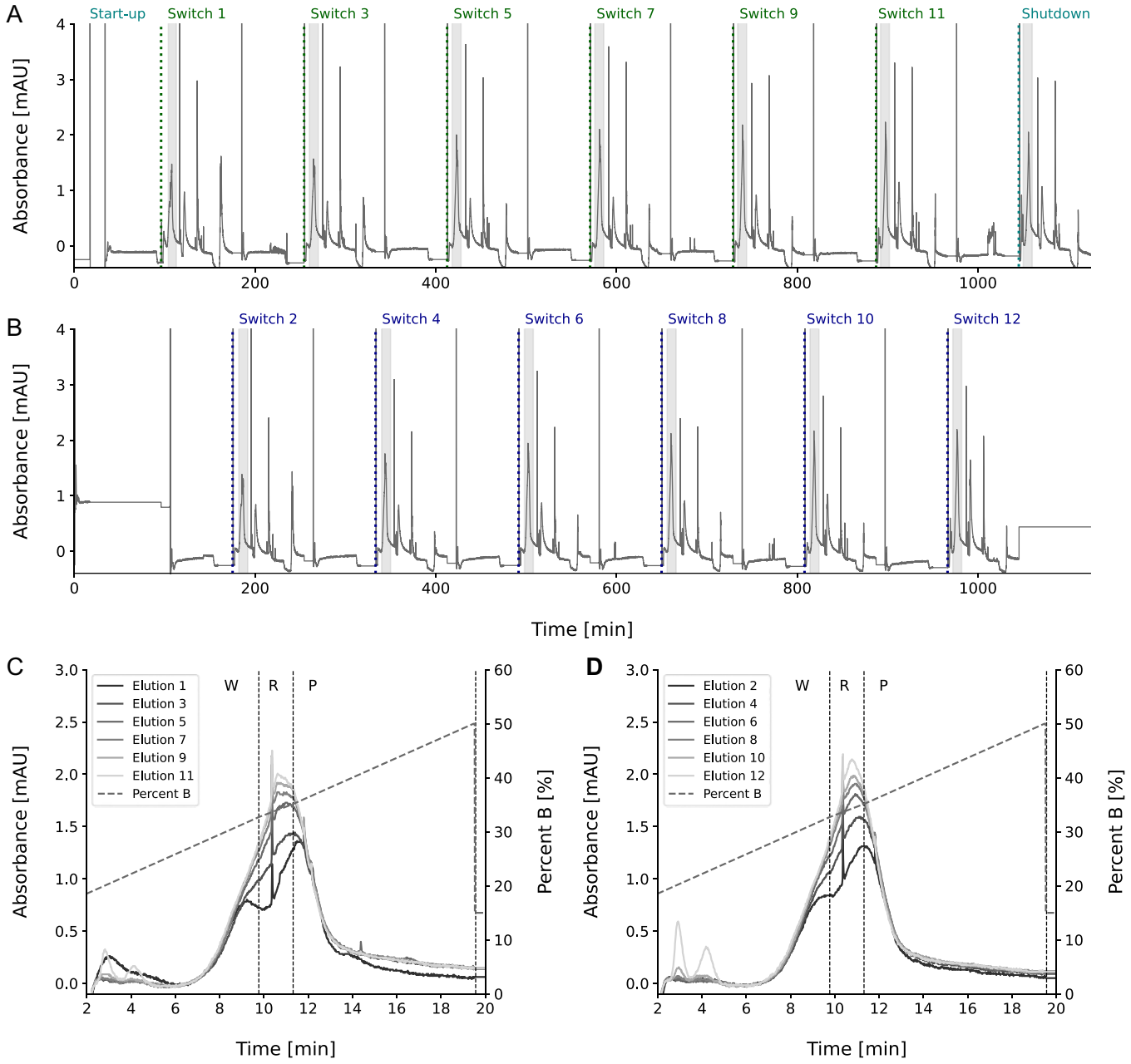

FIGURE 4 | MCSGP Run for the AAV2 full/empty separation. The entire MCSGP run, including the start-up and shut-down phase, for column 1 (A) and column 2 (B). The gradient elution phases are shaded in grey and the start of the individual phases indicated (blue: column 1 switches; green: column 2 switches; teal; start-up and shutdown). Superimposed elution peaks of column 1 (C) and column 2 (D). The gradient elution step is subdivided into the different phases of the MCSGP strategy: weakly adsorbing impurity out (W); recycling (R); product collection (P).

from the shutdown phase revealed that this fraction contained a full capsid content of 32% (data not shown). Additionally, the movement of the full AAV peak maximum to the left may be indicative of a mixture of species, not only containing empty and full, but also partial AAV particles. A possible hypothesis is that partially filled AAVs, whose retention time would be expected to overlap with the recycling region, could have accumulated over time. This could potentially have contributed to the observed accumulation and the seemingly moving peak maximum from right to left. The observed visual merging of the empty and full peak could therefore have been caused by a combination of several factors, an accumulation of full AAV and/or potentially partially filled AAVs.

Analysis of the final MCSGP pool showed that full AAV2 particles were enriched from 30.2% in the load to 67.7% (ddPCR) and from 27.2% to 61.1% (cryo-TEM) as shown in Table 2 and Figure 5. The MCSGP process was then compared with the batch chromatography by creating different mock pools (mock pools 1–3) from the design batch with different purities (Figure 6A). The mock pool 1 included the empty peak and therefore resulted in the lowest purity. The mock pool 2 reflects a yield-optimized scenario, where the recycled fractions containing the overlap of the weak impurities and the product (R) was included in the product pool. The mock pool 3 contained only the fractions of the product collection window (P), representing a purity-optimized pooling scenario.

TABLE 2 | Process performance parameters comparison for the batch mock pools (Figure 6A) and MCSGP polishing of AAV2 based on ddPCR and Cryo-TEM (Figure 5) analytics.

	ddPCR					Cryo-TEM					
			Productivity		Buffer consumption			Productivity		Buffer consumption	
	Yield	Full/empty ratio	total run [vg/L resin/h]	cycles [vg/L resin/h]	total run [L/vg]	cycles [L/vg]	Yield	Full/empty ratio	total run [full AAVs/L resin/h]	cycles [full AAVs/L resin/h]	total run [L/ full AAVs]	cycles [L/full]
	[%]	[% full]					[%]	[% full]				
MCSGP	74.4	67.7	1.7×10^{14}	1.8×10^{14}	12.0×10^{-14}	11.7×10^{-14}	79.1	61.1	1.5×10^{14}	1.6×10^{14}	13.3×10^{-14}	12.9×10^{-14}
Mock 2 (yield-optimized)	70.1	44.2	1.9×10^{14}		12.0×10^{-14}		79.9	45.4	2.0×10^{14}		12.3×10^{-14}	
Mock 3 (purity-optimized)	53.8	58.9	1.5×10^{14}		15.6×10^{-14}		61.4	60.6	1.5×10^{14}		16.1×10^{-14}	

For all four pools, the purity (full % calculated by ddPCR/ELISA and cryo-TEM/ELISA) and the yield (vector genome yield calculated by ddPCR/ELISA and the full AAV yield by cryo-TEM/ELISA) were calculated to assess the yield-purity relation. Figure 6B and C depict the yield versus purity relationship for different batch scenarios in comparison to the MCSGP process. This pareto plot demonstrates the relationship between the purity in dependence of the yield, which results in an inherent trade-off for batch chromatography when the product peak overlaps with adjacent impurity peaks (Figure 1). For the purity-optimized mock pool 3, a purity of 58.9% (ddPCR) and 60.6% (cryo-TEM) was achieved with a yield of 53.8% (ddPCR) and 61.4% (cryo-TEM), respectively. In comparison, in the yield-optimized mock pool 2 the yield was increased to 70.1% (ddPCR) and 79.9% (cryo-TEM). However, as typically observed in the batch gradient purification, this increase happened at the expense of purity, which decreased to 44.2% (ddPCR) and 45.4% (cryo-TEM). The MCSGP pool, in contrast, can maintain a comparable purity of 67.7% (ddPCR) and 61.1% (cryo-TEM) and at the same time increase the yield to 74.4% (ddPCR) and 79.1% (cryo-TEM) as depicted in Figure 6. That means for a comparable purity, MCSGP is able to increase the yield by 20.6% (ddPCR) and 17.6% (cryo-TEM) compared to the batch scenario (Figure 6BC).

Lastly, a process performance comparison was performed. In the start-up phase, the columns were equilibrated and the same quantity of feed as in the batch run was loaded. The shutdown serves to recover the last product from the column, without recycling the overlapping fraction, corresponding to a regular batch elution. Since no product is recovered from the start-up phase and during the shutdown, the product recovery corresponds to the same as in a batch chromatography.These phases generally have a negative impact on productivity and buffer consumption. Therefore, it is recommended to run a higher number of cycles to leverage the advantage of continuous twin-column chromatography and maximize process performance. The two process performance parameters, productivity and buffer consumption were calculated for the MCSGP pool and compared to the yield (mock pool 2) and purity-optimized (mock pool 3). As a worst case, the parameters were calculated for the total run, including the start-up and shutdown phase, and for the best-case scenario, they were evaluated for the cyclic phase, which is representative of continuous operation. The productivity and buffer consumption were calculated for the vg by ddPCR and for the full AAVs by cryo-TEM/ELISA (Table 2).

Compared to the yield-optimized batch (mock batch 2), there was little or no benefit in terms of productivity increase or buffer reduction. However, since the purity of the pool in mock batch 2 is much lower, the comparison to the purity-optimized batch (mock batch 3), which reaches similar purities, is more relevant. For this scenario, an increase in productivity and a reduced buffer consumption were observed even though only 6 cycles were performed. Compared to the yield-optimized batch, the productivity of MCSGP calculated by cryo-TEM was slightly worse (−2%) for the total run but increased by 8% for the cyclic evaluation. When assessed by ddPCR measurements, the use of MCSGP resulted in increased productivity for both scenarios: a + 12% increase for the total run and a + 23% increase for the cyclic evaluation.

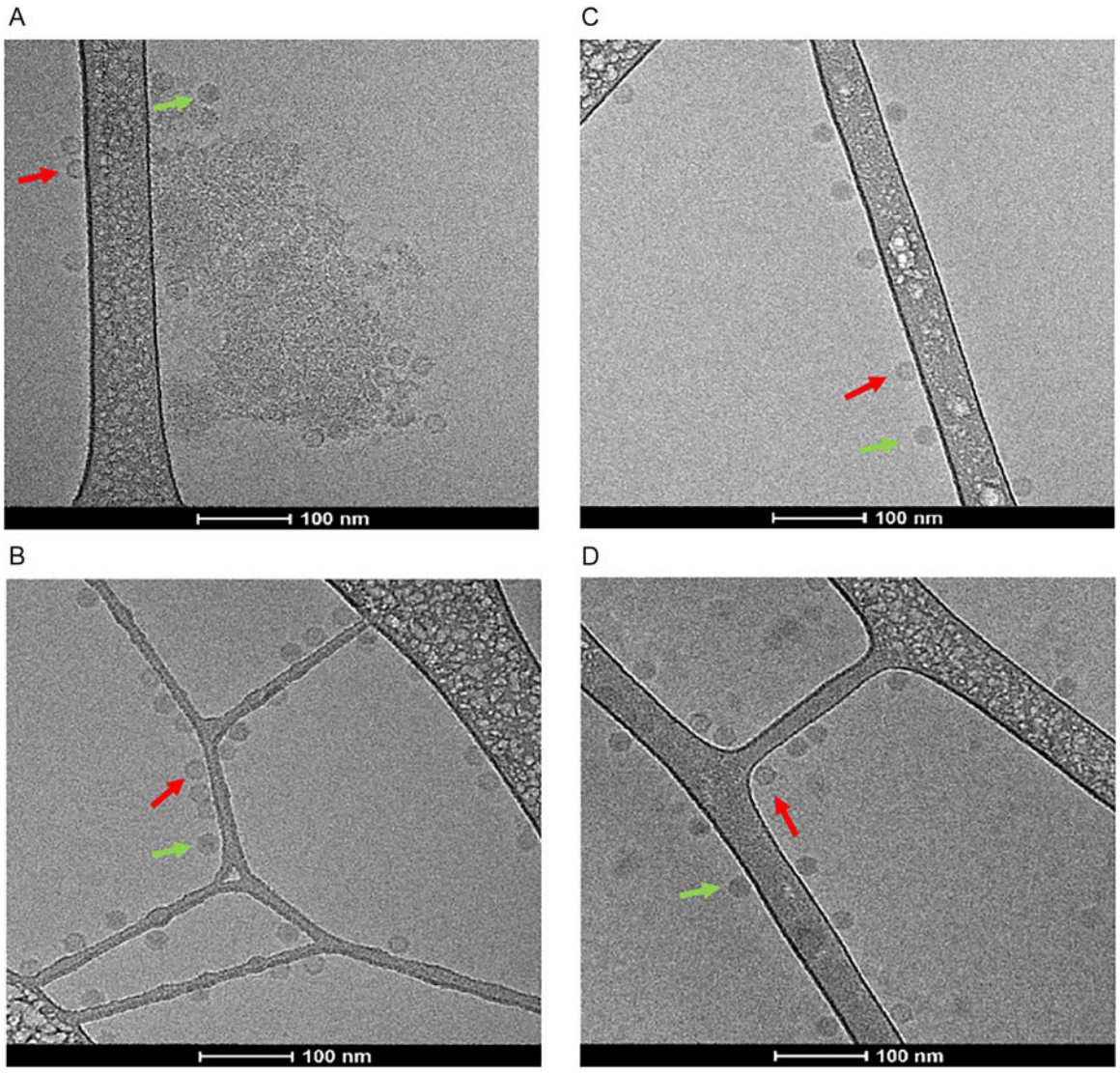

FIGURE 5 | Cryo-TEM analytics: Representative cryo-TEM images that were used to determine the full/empty ratio of the corresponding sample: (A) load; (B) yield-optimized mock pool; (C) purity-optimized mock pool; (D) MCSGP pool. Representative empty particles are indicated by a red arrow and full particles by a green arrow.

For the buffer usage, a reduced buffer consumption of up to −27% in the MCSGP run was observed with both analytical methods (Table 2). This improvement of process performance with only a low cycle number can be attributed to the beneficial rearranged time-scheduling that was possible due to omitting the strong recycling in the binary separation setting (Figure 3).

4 | Conclusion and Outlook

In this study, the potential of MCSGP to optimize the isolation of full AAV2 particles was investigated. The results demonstrated a successful enrichment of full AAV2 particles, increasing from 30.2% to 67.7% (ddPCR) and 27.2% to 61.1% (cryo-TEM) in the final MCSGP pool. Moreover, it was shown that applying MCSGP to AAV2 purification was able to circumvent the yield-purity trade-off and achieve a 20.6% (ddPCR) and 17.6% (cryo-TEM) higher yield as compared to a batch with comparable purity. Additionally, buffer consumption up to +27% (ddPCR) and +17% (cryo-TEM) and productivity was increased by up to +23% (ddPCR) and +8% (cryo-TEM). The latter was mainly attributed to the novel scheduling used to run MCSGP for a binary separation. To our knowledge, this is the first application of MCSGP for the preparative purification of AAVs. Based on this initial proof-of-concept, other adaptions as an improvement of the batch method to further increase purity and yield or the usage of alternative elution strategies, such as microstep- or isocratic elutions (Aebischer et al. 2022; Dickerson et al. 2021; Duzenli & Aslanidi 2025; Hejmowski et al. 2022; Joshi et al. 2021) may be considered for combination with MCSGP to further improve the isolation of full AAVs in the final polishing chromatography.

At the end of the purification process, it is vital to show that the activity of the AAVs was maintained and activity testing in the form of transduction experiments are planned in future studies. Overall, the results indicate the potential of MCSGP to serve as a scalable and robust technology, enabling higher yields, improved quality, and cost reduction in AAV and other viral vector purification processes.

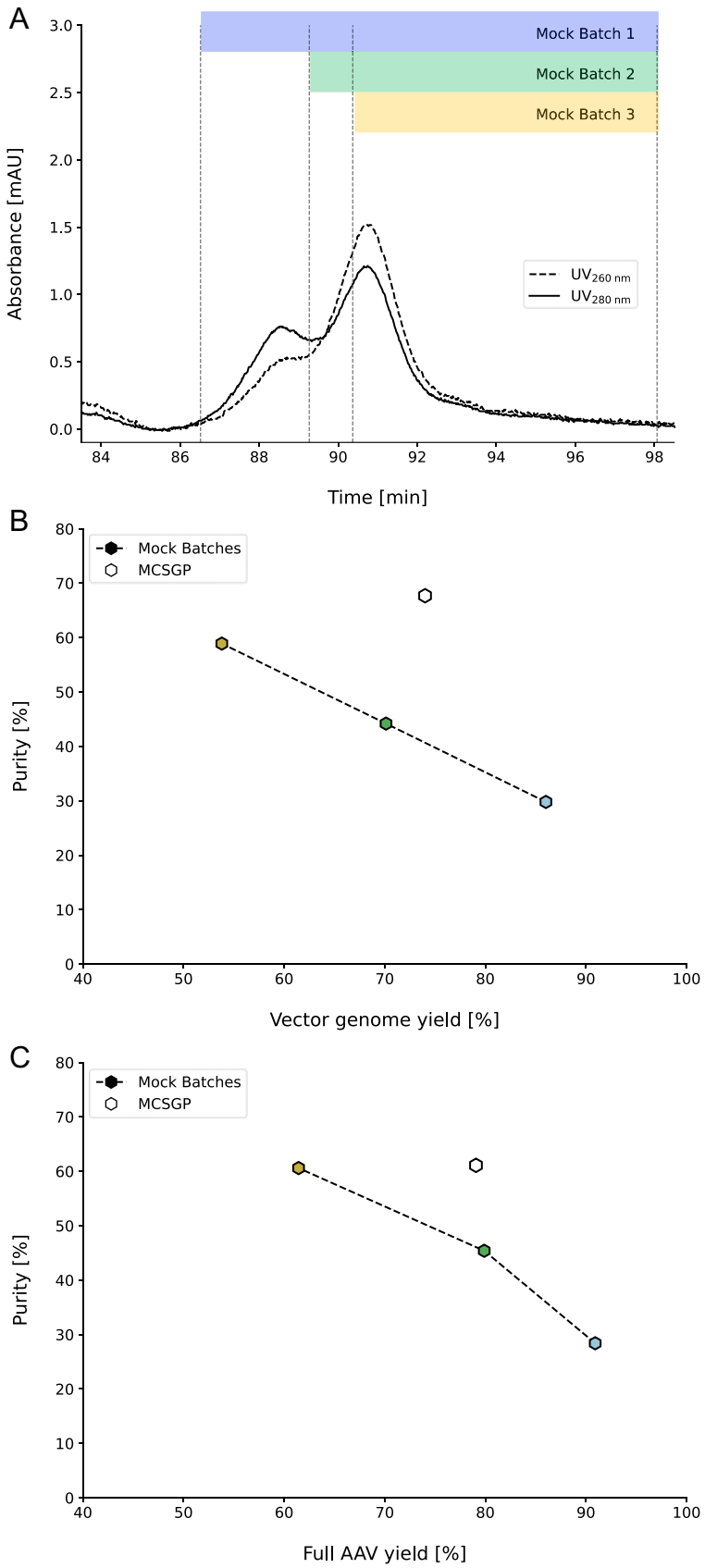

FIGURE 6 | Pareto curve for the comparison of batch vs MCSGP processes. (A) The fractions of the design batch were used to create three different mock batch pools. They were used for the purity and yield comparison with the MCSGP pool, to generate a pareto curve. The pareto curve was generated for (B) the purity and vg yield as calculated by ddPCR and (C) as purity and full AAV content as calculated by the cp titer (ELISA) combined with the full/empty ratio result (cryo- TEM). Blue: mock batch 1; green: mock batch 2; yellow: mock batch 3.

Author Contributions

Julia M. Müller: conceptualization, methodology, experimental work, data analysis and writing – original draft. **Tereza Müllerová:** methodology, experimental work, data analysis and writing – review and editing. **Daniela Tobler:** experimental work. **Damian Hauri:** experimental work, data analysis. **Richard Plieninger:** experimental work. **Yuki Higuchi:** conceptualization and writing – review and editing. **Ryosuke Takahashi:** conceptualization and writing – review and editing. **Sebastian Vogg:** conceptualization, methodology, experimental work and writing – review and editing **Thomas Müller-Späth:** conceptualization, project administration, funding acquisition, and writing – review and editing. **Thomas K. Villiger:** conceptualization, project administration, funding acquisition, and writing – review and editing.

Acknowledgments

We would like to thank the BioEM Lab of the Biozentrum, University of Basel, for their support with the Cryo-TEM imaging and the Protein Production and Structure Core Facility (PTPSP) at the EPFL Lausanne for granting us access to their mass photometer.

Conflicts of Interest

Y.H. and R.T. are employees of YMC CO., LTD., a company that sells continuous chromatography systems and the AEX columns used in this study. S.V. and T.M.S. are employees of ChromaCon AG, which sells continuous chromatography systems. ChromaCon AG has a licence for the MCSGP process patent and MCSGP-related patent applications pending. There is no other conflict of interest by any of the authors.

Data Availability Statement

The data that support the findings of this study are available from the corresponding author upon reasonable request.

References

Aebischer, M., H. Gizardin-Fredon, H. Lardeux, et al. 2022. "Anion-Exchange Chromatography at the Service of Gene Therapy: Baseline Separation of Full/Empty Adeno-AssociatedVirus Capsids by Screening of Conditions and Step Gradient Elution Mode." *International Journal of Molecular Sciences* 23, no. 20: 12332. https://doi.org/10.3390/ijms232012332.

Arjomandnejad, M., I. Dasgupta, T. R. Flotte, and A. M. Keeler. 2023. "Immunogenicity of Recombinant Adeno-Associated Virus (AAV) Vectors for Gene Transfer." *BioDrugs* 37, no. 3: 311–329. https://doi.org/10.1007/s40259-023-00585-7.

Chen, H. 2015. "Adeno-Associated Virus Vectors for Human Gene Therapy." *World Journal of Medical Genetics* 5, no. 3: 28. https://doi.org/10.5496/wjmg.v5.i3.28.

Coolbaugh, M. J., C. T. Varner, T. A. Vetter, et al. 2021. "Pilot-Scale Demonstration of an end-to-end Integrated and Continuous Biomanufacturing Process." *Biotechnology and Bioengineering* 118, no. 9: 3287–3301. https://doi.org/10.1002/bit.27670.

Dickerson, R., C. Argento, J. Pieracci, and M. Bakhshayeshi. 2021. "Separating Empty and Full Recombinant Adeno-Associated Virus Particles Using Isocratic Anion Exchange Chromatography." *Biotechnology Journal* 16, no. 1: 2000015. https://doi.org/10.1002/biot.202000015.

Duzenli, O. F., and G. Aslanidi. 2025. "Consecutive Affinity and Ion-Exchange Chromatog-Raphy for AAV9 Vectors Purification." *Biomedicines* 13, no. 2: 361. https://doi.org/10.3390/biomedicines13020361.

Ebberink, E., A. Ruisinger, M. Nuebel, M. Thomann, and A. Heck. 2022. "Assessing Production Variability in Empty and Filled Adeno-Associated Viruses by Single Molecule Mass Analyses." *Molecular Therapy. Methods & Clinical Development* 27: 491–501. https://doi.org/10.1016/j.omtm.2022.11.003.

El Andari, J., and D. Grimm. 2021. "Production, Processing, and Characterization of Synthetic AAV Gene Therapy Vectors." *Biotechnology Journal* 16, no. 1: 2000025. https://doi.org/10.1002/biot.202000025.

FDA. (2010). "Guidance for Industry: Characterization and Qualification of Cell Substrates and Other Biological Materials Used in the Production of Viral Vaccines for Infectious Disease Indications." Biotechnology Law Report.

Fu, Q., A. Polanco, Y. S. Lee, and S. Yoon. 2023. "Critical Challenges and Advances in Recombinant Adeno-Associated Virus (rAAV) Biomanufacturing." *Biotechnology and Bioengineering* 120, no. 9: 2601–2621. https://doi.org/10.1002/bit.28412.

Gagnon, P., B. Goričar, S. D. Prebil, H. Jug, M. Leskovec, and A. Štrancar (2021). "Separation of Empty and Full Adeno-Associated Virus Capsids From a Weak Anion Exchanger by Elution With an Ascending pH Gradient at Low Ionic Strength." *BioProcessing Journal* 20. https://doi.org/10.12665/J20OA.Gagnon.

Gimpel, A. L., G. Katsikis, and S. Sha, et al. 2021. "Analytical Methods for Process and Product Characterization of Recombinant Adeno-Associated Virus-Based Gene Therapies." *Molecular Therapy Methods & Clinical Development* 20: 740–754. https://doi.org/10.1016/j.omtm.2021.02.010.

Grieger, J. C., V. W. Choi, and R. J. Samulski. 2006. "Production and Characterization of Adeno-Associated Viral Vectors." *Nature Protocols* 1, no. 3: 1412–1428. https://doi.org/10.1038/nprot.2006.207.

Hejmowski, A. L., K. Boenning, J. Huato, A. Kavara, and M. Schofield. 2022. "Novel Anion Exchange Membrane Chromatography Method for the Separation of Empty and Full Adeno-Associated Virus." *Biotechnology Journal* 17, no. 2: 2100219. https://doi.org/10.1002/biot.202100219.

Henry, O., E. Dormond, M. Perrier, and A. Kamen. 2004. "Insights Into Adenoviral Vector Production Kinetics in Acoustic Filter-Based Perfusion Cultures." *Biotechnology and Bioengineering* 86, no. 7: 765–774. https://doi.org/10.1002/bit.20074.

Hermens, W. T. J. M. C., O. T. Brake, P. A. Dijkhuizen, et al. 1999. "Purification of Recombinant Adeno-Associated Virus by Iodixanol Gradient Ultracentrifugation Allows Rapid and Reproducible Preparation of Vector Stocks for Gene Transfer in the Nervous System." *Human Gene Therapy* 10, no. 11: 1885–1891. https://doi.org/10.1089/10430349950017563.

Issa, S. S., A. A. Shaimardanova, V. V. Solovyeva, and A. A. Rizvanov. 2023. "Various AAV Serotypes and Their Applications in Gene Therapy: An Overview." *Cells* 12, no. 5: 785. https://doi.org/10.3390/cells12050785.

Jarvi, N., K. Hofman, A. Venkatesh, E. Gorecki, and S. V. Balu-Iyer. 2024. "Immunogenicity Risk Assessment of Empty Capsids Present in Adeno-Associated Viral Vectors Using Predictive Innate Immune Responses." *Journal of Pharmaceutical Sciences* 113: S00223549 24004106. https://doi.org/10.1016/j.xphs.2024.09.006.

Jiang, Z., and P. A. Dalby. 2023. "Challenges in Scaling up AAV-Based Gene Therapy Manufacturing." *Trends in Biotechnology* 41, no. 10: 1268–1281. https://doi.org/10.1016/j.tibtech.2023.04.002.

Joshi, P. R. H., A. Bernier, P. D. Moço, J. Schrag, P. S. Chahal, and A. Kamen. 2021. "Development of a Scalable and Robust AEX Method for Enriched rAAV Preparations in Genome-Containing VCs of Serotypes 5, 6, 8, and 9." *Molecular Therapy - Methods & Clinical Development* 21: 341–356. https://doi.org/10.1016/j.omtm.2021.03.016.

Jungbauer, A. 2013. "Continuous Downstream Processing of Biopharmaceuticals." *Trends in Biotechnology* 31, no. 8: 479–492. https://doi.org/10.1016/j.tibtech.2013.05.011.

Khanal, O., V. Kumar, and M. Jin. 2023. "Adeno-Associated Viral Capsid Stability on Anion Exchange Chromatography Column and Its Impact on Empty and Full Capsid Separation." *Molecular Therapy. Methods & Clinical Development* 31: 101112. https://doi.org/10.1016/j.omtm.2023.101112.

Kurth, S., T. Li, A. Hausker, et al. 2024. "Separation of Full and Empty Adeno-Associated Virus Capsids by Anion-Exchange Chromatography Using Choline-Type Salts." *Analytical Biochemistry* 686: 115421. https://doi.org/10.1016/j.ab.2023.115421.

Lam, A. K., P. L. Mulcrone, D. Frabutt, et al. 2023. "Comprehensive Comparison of AAV Purification Methods: Iodixanol Gradient Centrifugation vs. Immuno-Affinity Chromatography." *Advances in Cell and Gene Therapy* 2023: 1–12. https://doi.org/10.1155/2023/2339702.

Lavoie, R. A., J. T. Zugates, A. T. Cheeseman, et al. 2023. "Enrichment of Adeno-Associated Virus Serotype 5 Full Capsids by Anion Exchange Chromatography With Dual Salt Elution Gradients." *Biotechnology and Bioengineering* 120, no. 10: 2953–2968. https://doi.org/10.1002/bit.28453.

Lock, M., M. Alvira, L. H. Vandenberghe, et al. 2010. "Rapid, Simple, and Versatile Manufacturing of Recombinant Adeno-Associated Viral Vectors at Scale." *Human Gene Therapy* 21, no. 10: 1259–1271. https://doi.org/10.1089/hum.2010.055.

Luca, C. D., S. Felletti, G. Lievore, et al. 2020. "From Batch to Continuous Chromatographic Purification of a Therapeutic Peptide Through Multicolumn Countercurrent Solvent Gradient Purification." *Journal of Chromatography A* 1625: 461304. https://doi.org/10.1016/j.chroma.2020.461304.

Mendes, J. P., M. Bergman, A. Solbrand, C. Peixoto, M. J. T. Carrondo, and R. J. S. Silva. 2022. "Continuous Affinity Purification of Adeno-Associated Virus Using Periodic Counter-Current Chromatography." *Pharmaceutics* 14, no. 7: 1346. https://doi.org/10.3390/pharmaceutics14071346.

Mendes, J. P., B. Fernandes, E. Pineda, et al. 2022. "AAV Process Intensification by Perfusion Bioreaction and Integrated Clarification." *Frontiers in Bioengineering and Biotechnology* 10: 1020174. https://doi.org/10.3389/fbioe.2022.1020174.

Moleirinho, M. G., R. J. S. Silva, P. M. Alves, M. J. T. Carrondo, and C. Peixoto. 2020. "Current Challenges in Biotherapeutic Particles Manufacturing." *Expert Opinion on Biological Therapy* 20, no. 5: 451–465. https://doi.org/10.1080/14712598.2020.1693541.

Müller-Späth, T., M. Krättli, L. Aumann, G. Ströhlein, and M. Morbidelli. 2010. "Increasing the Activity of Monoclonal Antibody Therapeutics by Continuous Chromatography (MCSGP)." *Biotechnology and Bioengineering* 107, no. 4: 652–662. https://doi.org/10.1002/bit.22843.

Nass, S. A., M. A. Mattingly, D. A. Woodcock, et al. 2018. "Universal Method for the Purification of Recombinant AAV Vectors of Differing Serotypes." *Molecular Therapy. Methods & Clinical Development* 9: 33–46. https://doi.org/10.1016/j.omtm.2017.12.004.

O'Connor, D. M., C. Lutomski, M. F. Jarrold, N. M. Boulis, and A. Donsante. 2019. "Lot-to-lot Variation in Adeno-Associated Virus Serotype 9 (AAV9) Preparations." *Human Gene Therapy Methods* 30, no. 6: 214–225. https://doi.org/10.1089/hgtb.2019.105.

Park, D., T. N. T. Nguyen, J. Sangerman, et al. 2024. "Continuous Production of Recombinant Adeno-Associated Viral Vectors via Transient Transfection of HEK293 Cells in Perfusion Bioreactor." *Computer Aided Chemical Engineering* 53: 2587–2592. https://doi.org/10.1016/B978-0-443-28824-1.50432-4.

Penaud-Budloo, M., A. François, N. Clément, and E. Ayuso. 2018. "Pharmacology of Recombinant Adeno-Associated Virus Production." *Molecular Therapy. Methods & Clinical Development* 8: 166–180. https://doi.org/10.1016/j.omtm.2018.01.002.

Qu, G., J. Bahr-Davidson, J. Prado, et al. 2007. "Separation of Adeno-Associated Virus Type 2 Empty Particles From Genome Containing Vectors by Anion-Exchange Column Chromatography." *Journal of Virological Methods* 140, no. 1–2: 183–192. https://doi.org/10.1016/j.jviromet.2006.11.019.

Ramos, I., N. Sharda, R. Villafana, et al. 2023. "Fully Integrated Downstream Process to Enable Next-Generation Manufacturing." *Biotechnology and Bioengineering* 120, no. 7: 1869–1881. https://doi.org/10.1002/bit.28384.

Rieser, R., J. Koch, G. Faccioli, et al. 2021. "Comparison of Different Liquid Chromatography-Based Purification Strategies for Adeno-Associated Virus Vectors." *Pharmaceutics* 13, no. 5: 748. https://doi.org/10.3390/pharmaceutics13050748.

Steinebach, F., N. Ulmer, L. Decker, L. Aumann, and M. Morbidelli. 2017. "Experimental Design of a Twin-Column Countercurrent Gradient Purification Process." *Journal of Chromatography A* 1492: 19–26. https://doi.org/10.1016/j.chroma.2017.02.049.

Strobel, B., F. D. Miller, W. Rist, and T. Lamla. 2015. "Comparative Analysis of Cesium Chloride- and Iodixanol-Based Purification of Recombinant Adeno-Associated Viral Vectors for Preclinical Applications." *Human Gene Therapy Methods* 26, no. 4: 147–157. https://doi.org/10.1089/hgtb.2015.051.

Tanaka, T., H. Hanaoka, and S. Sakurai. 2020. "Optimization of the Quality by Design Approach for Gene Therapy Products: A Case Study for Adeno-Associated Viral Vectors." *European Journal of Pharmaceutics and Biopharmaceutics* 155: 88–102. https://doi.org/10.1016/j.ejpb.2020.08.002.

Urabe, M., K.-Q. Xin, Y. Obara, et al. 2006. "Removal of Empty Capsids From Type 1 Adeno-Associated Virus Vector Stocks by Anion-Exchange Chromatography Potentiates Transgene Expression." *Molecular Therapy* 13, no. 4: 823–828. https://doi.org/10.1016/j.ymthe.2005.11.024.

Venkatakrishnan, B., J. Yarbrough, J. Domsic, et al. 2013. "Structure and Dynamics of Adeno-Associated Virus Serotype 1 VP1-Unique N-Terminal Domain and Its Role in Capsid Trafficking." *Journal of Virology* 87, no. 9: 4974–4984. https://doi.org/10.1128/JVI.02524-12.

Wada, M., N. Uchida, G. Posadas-Herrera, et al. 2023. "Large-Scale Purification of Functional AAV Particles Packaging the Full Genome Using Short-Term Ultracentrifugation With a Zonal Rotor." *Gene Therapy* 30, no. 7–8: 641–648. https://doi.org/10.1038/s41434-023-00398-x.

Wang, C., S. Mulagapati, Z. Chen, et al. 2019. "Developing an Anion Exchange Chromatography Assay for Determining Empty and Full Capsid Contents in Aav6.2." *Molecular Therapy. Methods & Clinical Development* 15: 257–263. https://doi.org/10.1016/j.omtm.2019.09.006.

Weldon, R., J. Lill, M. Olbrich, P. Schmidt, and T. Müller-Späth. 2022. "Purification of a GalNAc-Cluster-Conjugated Oligonucleotide by Reversed-Phase Twin-Column Continuous Chromatography." *Journal of Chromatography A* 1663: 462734. https://doi.org/10.1016/j.chroma.2021.462734.

Wright, J. 2014. "Product-Related Impurities in Clinical-Grade Recombinant AAV Vectors: Characterization and Risk Assessment." *Biomedicines* 2, no. 1: 80–97. https://doi.org/10.3390/biomedicines2010080.

Wright, J. F. 2008. "Manufacturing and Characterizing AAV-Based Vectors for Use in Clinical Studies." *Gene Therapy* 15, no. 11: 840–848. https://doi.org/10.1038/gt.2008.65.

Wright, J. F., T. Le, J. Prado, et al. 2005. "Identification of Factors That Contribute to Recombinant AAV2 Particle Aggregation and Methods to Prevent Its Occurrence During Vector Purification and Formulation." *Molecular Therapy* 12, no. 1: 171–178. https://doi.org/10.1016/j.ymthe.2005.02.021.

Zolotukhin, S., B. J. Byrne, E. Mason, et al. 1999. "Recombinant Adeno-Associated Virus Purification Using Novel Methods Improves Infectious Titer and Yield." *Gene Therapy* 6, no. 6: 973–985. https://doi.org/10.1038/sj.gt.3300938.

Supporting Information

Additional supporting information can be found online in the Supporting Information section.